Journal of Mechanical Science and Technology, Vol. 19, No. 1, ⟨Special Edition⟩ pp. 255~264, 2005 255

Vehicle Dynamic Simulation Including an Artificial Neural Network Bushing Model

Jeong Hyun Sohn*
Department of Mechanical Engineering,
Pukyong National University, Busan 608-739, Korea
Woon Kyung Baek
Department of Mechanical Engineering,
Pukyong National University, Busan 608-739, Korea

In this paper, a practical bushing model is proposed to improve the accuracy of the vehicle dynamic analysis. The results of the rubber bushing are used to develop an empirical bushing model with an artificial neural network. A back propagation algorithm is used to obtain the weighting factor of the neural network. Since the output for a dynamic system depends on the histories of inputs and outputs, Narendra algorithm of 'NARMAX' form is employed to consider these effects. A numerical example is carried out to verify the developed bushing model. Then, a full car dynamic model with artificial neural network bushings is simulated to show the feasibility of the proposed bushing model.

Key Words : Vehicle Dynamics, Bushing, Neural Network, Simulation

1. Introduction

The multi-body dynamic analysis techniques using high-performance computers have been effective tools for the analysis and design in the machine and automobile industries. Among these techniques, commercial programs such as DADS and ADAMS have been often used (CADSI, 1995; ADAMS, 1994).

Vehicle dynamic simulation can be used to estimate the vehicle characteristics such as the ride quality and the component durability. However, modeling of the rubber bushing elements has been obstacles to degrade the qualities of the dynamic simulation results. The bushing element shows nonlinear characteristics for both in load amplitudes and frequencies, and also hysteretic responses for the repeated vibrational excitations. Since the characteristics of the rubber bushing affects significantly to the accuracy of the vehicle dynamic simulation result, it should be accurately considered in the vehicle suspension model.

Blundell (1998) used a joint model, a linear/non-linear bushing model to describe the influence of rubber bush compliance on vehicle suspension movements. He showed that the bushing element should be included for the accurate vehicle dynamic simulation. The commercial multi-body dynamic analysis programs usually adopt the Kelvin-Voight model for the bushing element. This model simply treats the bushing element as the linear combination of translational/rotational spring-dampers. However, this type of bushing model cannot generate the hysteretic behavior of the bushing element.

Recently, artificial neural network algorithm is introduced in modeling shock absorbers. Fash (1994) used the neural network algorithm to

* Corresponding Author,
E-mail : jhsohn@pknu.ac.kr
TEL : +82-51-620-1539; **FAX** : +82-51-620-1405
Department of Mechanical Engineering, Pukyong National University, Busan 608-739, Korea. (Manuscript **Received** November 29, 2004; **Revised** December 15, 2004)

model the behavior of the shock absorber and Kim (1995) used it to model the vehicle suspension system. Recently Barber (2000) suggested the possibility of the artificial neural network for modeling the bush.

In this paper, a new bushing model using the neural network algorithm is proposed to take into consideration for both the hysteresis and the nonlinearities of frequency and displacement of the rubber based on the dynamic test results of the rubber bushing elements. A MTS testing machine, which is an one-axis durability tester, is used to capture the practical dynamic behavior of the bushing. The new bushing model using the neural network is suggested in chapter 2 and experimental procedure and test result of the bushing element are described in chapter 3. In chapter 4, the new bushing model is verified using a numerical example and a full-car model is demonstrated using this new bushing model in chapter 5.

2. A New Bushing Model

2.1 Artificial neural network

A multi-perceptron neuron structure of the artificial neural network consists of the input layer, the hidden layer, and the output layer. Fig. 1 shows a general perceptron neural structure. To predict the time response of the dynamical systems using the artificial neural network, the hyperbolic tangent sigmoid function is usually employed as following,

$$y=\tanh ax \tag{1}$$

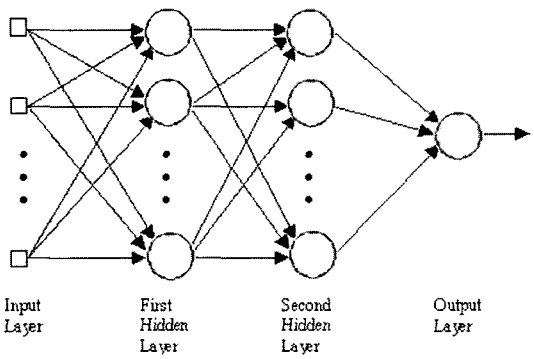

Fig. 1 Perceptron neural structure

where x is the input, y is the output, and a is the parameter for adjusting the gradient of the curve.

2.2 Construction of the neural network for the rubber bushing model

Since the rubber bush has hysteretic characteristics, the inputs and outputs of the previous steps affect the current outputs. Therefore, inputs and outputs of the past are used as the input data of the current step. The input components of the neural network are selected from the current displacement and velocity, the past displacement and the velocity, and the past outputs. The value of the output layer is the rubber bush force. The hidden layer composed of two layers. Through a trial-and-error process, the first hidden layer was assigned with 10 nodes and the second hidden layer was assigned with 9 nodes. Figure 2 shows the structure of the neural network used in this study. The relation between the input and the output is represented by the following equation, which is known as 'NARMAX form' (Narendra and Parthasarathy, 1990);

$$y_k=f(u_k, u_{k-1}, \cdots, u_{k-m}, y_{k-1}, \cdots, y_{k-N}) \tag{2}$$

where y_k represents the output of k-th pattern, u_k is the input of k-th pattern, m indicates the number of previous input data, and N means the number of pre-step output.

In this study, the rubber bush characteristics were measured using MTS 244.12 machine. The

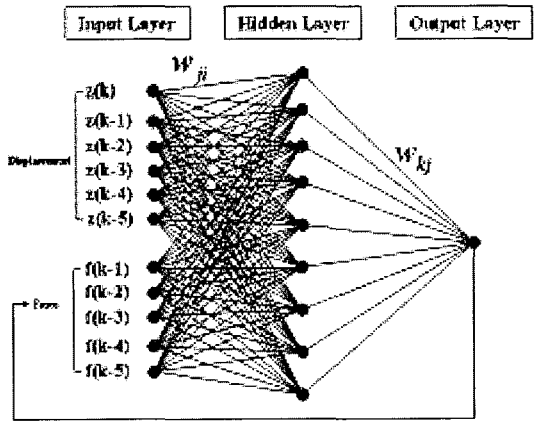

Fig. 2 Structure of the neural network used in this study

force data corresponding to the displacement of the rubber bush were obtained by using RPCIII software installed in the machine. The deformation and the force were normalized before being used as the input data for the neural network. Then, the value of the input data is divided by the maximum value of the input data and processed by the hyperbolic tangent sigmoid function. To obtain the appropriate weighting factors, the artificial neural network is trained by using the experimental result under the random excitation.

2.3 Implementation of the neural network bushing model in ADAMS

The neural network model requires input data at a fixed sampling rate. Also, it requires the information of the past input and output at each integration time step. Since the dynamic analysis program like ADAMS uses a variable step integration algorithm and the intermediate data are not available for the user, the following steps are required for the complete dynamic analysis using the bushing model.

(a) The sampling rate of the dynamic analysis needs to be adjusted to coincide with that of the neural network.

(b) The current step is verified whether it has achieved the convergence state or not.

(c) The input and output of the past event are saved in the buffer.

The numerical algorithm to calculate the forces of the rubber bush in the current step can be developed by the following sequence :

(a) The rubber bush characteristics data is obtained from the experiment using testing machine.

(b) The weighting factors of the neural network is obtained from the neural network learning and saved in the file.

(c) Read the weighting factors in the neural network bushing model subroutine.

(d) The weighting factors are arranged in the layer.

(e) The rubber bush deformation and deformation rate in the current step are calculated.

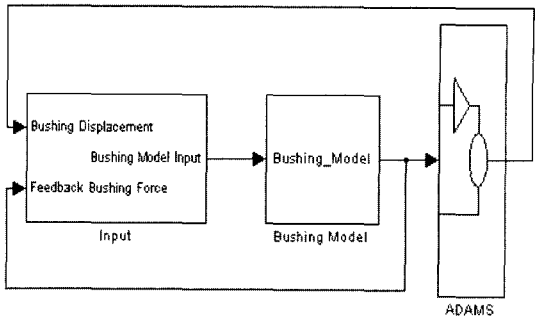

Fig. 3 Bushing model using MATLAB and ADAMS

The bushing model using the neural network algorithm was developed using MATLAB (Richard, 2003). An interface module between the neural network bushing model and ADAMS program was also implemented. SIMULINK (Richard, 2003) was used to link MATLAB and ADAMS as shown in Fig. 3. Under the SIMULINK environment, ADAMS produces bushing deformation data and these data are transferred to MATLAB. Then, MATLAB calculates bushing force data and these data are used for the next time step in ADAMS.

In the dynamics simulation, the bushing force calculated using the neural net algorithm can be transmitted to each body through the following procedure.

(a) The current displacement, the current output force, and the past displacement need to be entered into the neural network for calculating the rubber bush force at the current time step.

(b) The rubber bush force is changed into the force and moment acting at the center of the mass of the body connected to the rubber bush.

(c) The current displacement and force data are saved in the buffer for the calculation at the next time step.

3. Experiments to Capture the Bushing Characteristics

3.1 Test Rig

All the bushing tests were conducted by an one-axis MTS testing machine. The specifications of the machine are shown in the Table 1. A test

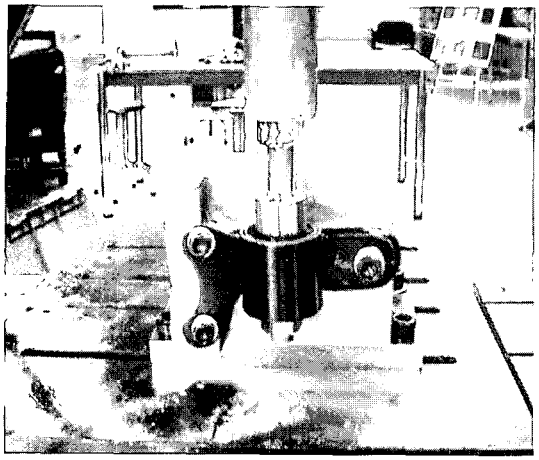

(a) Test in the axial direction

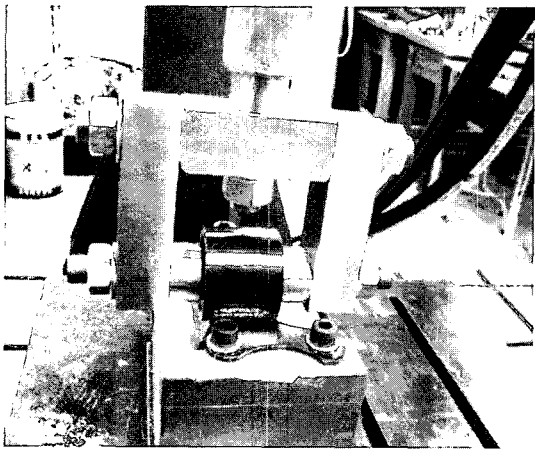

(b) Test in the radial direction

Fig. 4 Test rig for the bushing element

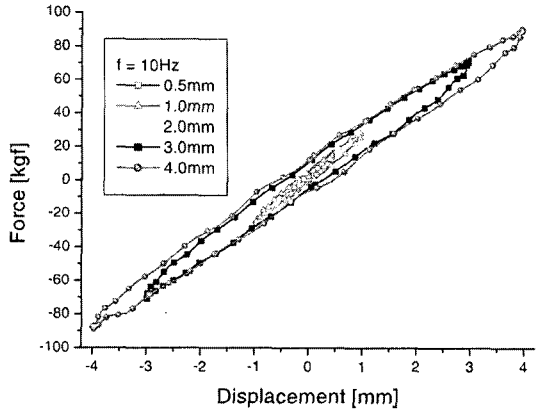

Fig. 5 Axial bushing force (10 hz sine wave)

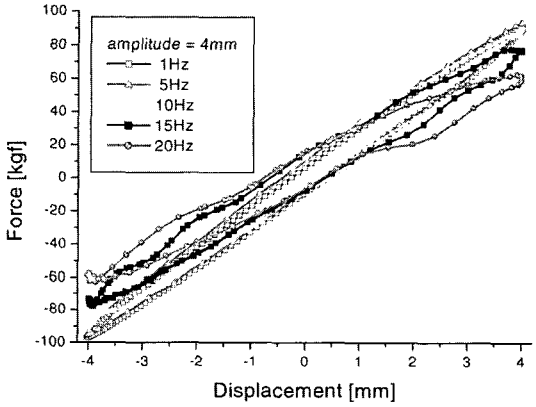

Fig. 6 Axial bushing force (4 mm, sine wave)

rig was constructed to hold the bushing element and is shown in Figure 4.

3.2 Test results

3.2.1 Harmonic tests

The purpose of the tests was to determine the bushing stiffness and damping characteristics as a function of vibration amplitude and frequency when the bushing is loaded in the displacement range where normally experiences in proving ground durability tests. The harmonic tests were conducted using sinusoidal vibration wave form. The tests were carried out with five different frequencies, that is, 1, 5, 10, 15, and 20 Hz. The corresponding amplitudes were, 0.5, 1.0, 2.0, 3.0, and 4.0 mm, respectively. The loads were applied both in axial and radial directions. Since the power spectral density of the bushing load measured from the proving ground test durability analysis typically exhibits a peak value in the range of 10–15 Hz, the maximum frequency for the test was conservatively set at 20 Hz. The forces on the rubber bush due to the change of the amplitude and the frequency were measured for duration of 10 seconds. The resulting forces in the axial direction are shown in the Fig. 5 and Fig. 6 and those of radial direction are represented in Fig. 7 and Fig. 8, respectively. Figure 5 shows the axial bushing force due to the sine wave excitation at 10 Hz. The more amplitude increases, the higher bushing force becomes. Figure 6 shows the axial bushing force due to the sine wave excitation with the amplitude of 4 mm. The

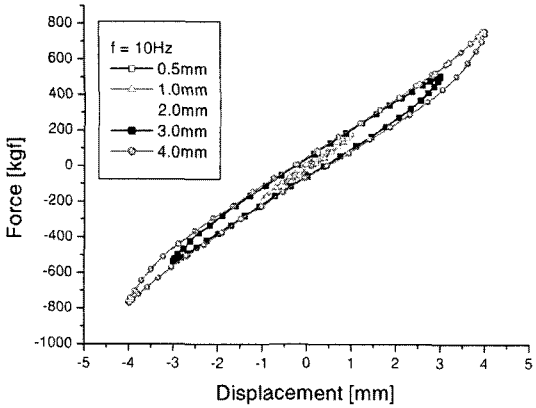

Fig. 7 Radial bushing force (10 hz sine wave)

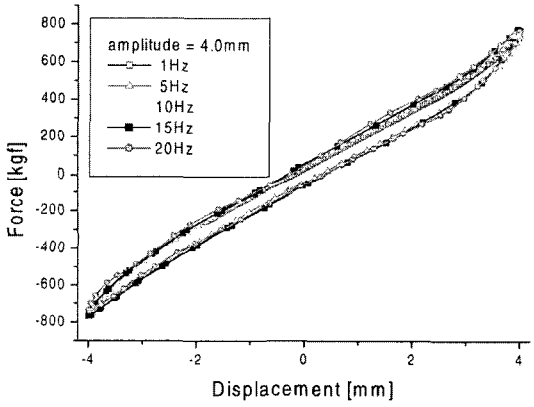

Fig. 8 Radial bushing force (4 mm, sine wave)

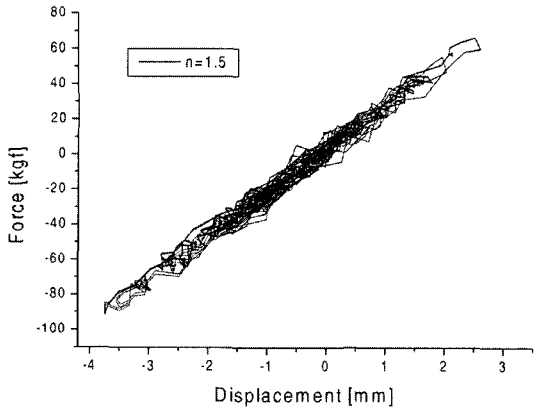

Fig. 9 Axial bushing force under the random input

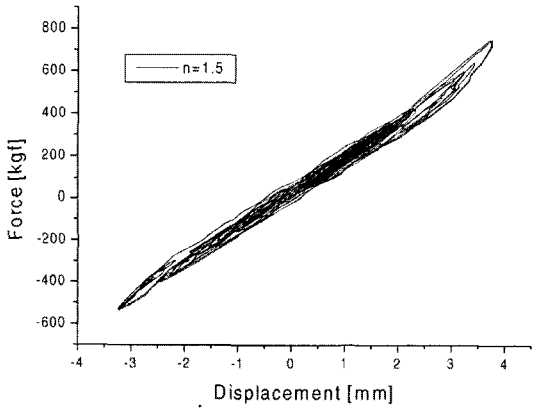

Fig. 10 Radial bushing force under the random input

more frequency increases, the softer bushing stiffness becomes. Figure 7 and Figure 8 are the radial bushing forces and show similar results as Fig. 5 and Fig. 6 However, the radial bushing results show a considerable nonlinear tendency of the bushing.

3.2.2 Random tests

The random input data were generated by using RPCIII software supported by MTS, Inc. The RPCIII system has the following sampling rates, i.e., 51.2, 64, 102.4, 204.8, 256, 409.6, 512, 1024, 2048 Hz. Since a sampling rate of 204.8 Hz was chosen with a frame size of 1024 points per frame, the time interval was calculated as 0.0049. The amplitude of random data profile is changed according to the index 'n'. The axial and radial bushing forces measured from the experiments when index 'n' is 1.5 are shown in Figure 9 and 10, respectively. Figure 9 show the linear tendency in the axial direction of the bushing and Figure 10 represents the nonlinear dynamic characteristic in the radial direction of the bushing, respectively.

4. Verification of the Neural Network Bushing Model

A dynamic model of the test rig was constructed to verify the empirical bushing model using the artificial neural network. ADAMS program was used to construct the empirical bushing model as shown in Fig. 11. A bushing element was installed between the ground and the excitation device. The excitation device was connected to

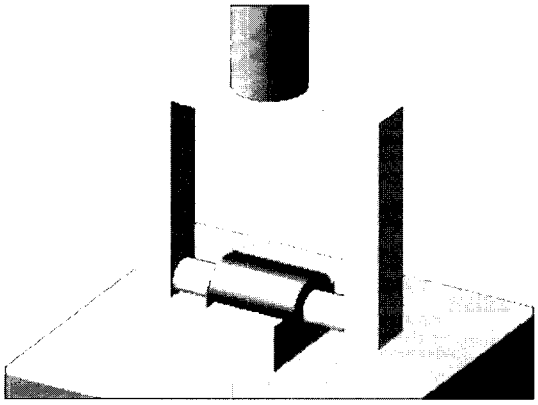

Fig. 11 Dynamic model of the bushing test rig using ADAMS

the ground with a translational joint. The random input was imposed on the translational joint to generate the motion. The random input signal and the calculated output with an exponent index of value of 'n' equals to 1.0 are shown in the Fig. 12 and Fig. 13, respectively. In the Fig. 13, the solid line represents the test result and the dashed line represents the simulation result from ADAMS. Although there are some differences in the peak values, it can be noted that the weighting factor is learning well to follow the optimal fit. Figure 14 and Figure 15 show the random input data and the result with different exponential index of value 'n' equal to 1.5. The simulation results show a good agreement with the test results.

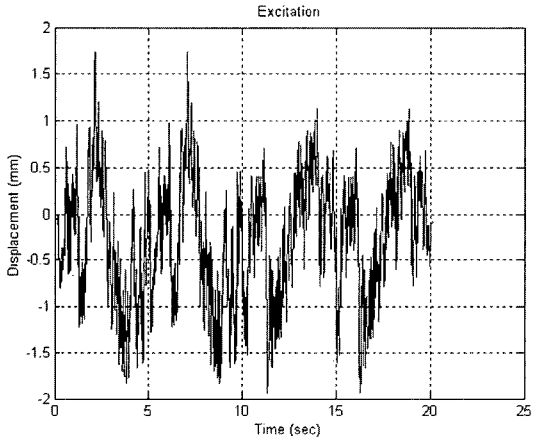

Fig. 12 Random input excitation for neural network learning with index value 'n'=1

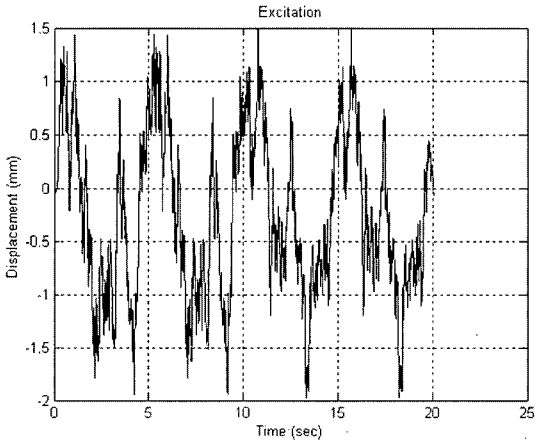

Fig. 14 Random input data for verification with index value 'n'=1.5

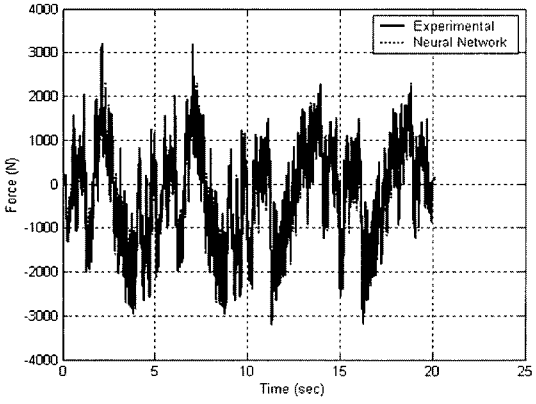

Fig. 13 Bushing force from the random input with index value 'n'=1

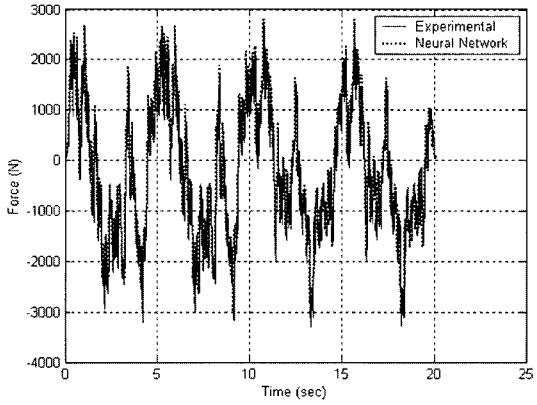

Fig. 15 Bushing force with index value 'n'=1.5

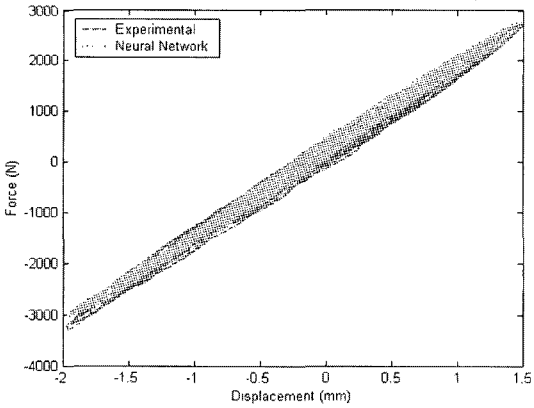

Fig. 16 Comparison of displacements vs. bushing forces

Figure 16 shows the displacement versus bushing force. It shows that the simulation result predicts the hysteretic response of the bushing very well.

5. Vehicle Dynamic Analysis Using Neural Network Bushing Model

5.1 Full-car simulation

To demonstrate the proposed bushing model, a full-car model was used as shown in Fig. 17. The front suspension is McPherson strut type suspension and a rear suspension is a torsion beam type suspension. A damper of rear suspension is connected to the trailing arm with a bushing and also connected to the chassis with a spherical joint. The neural network bushing model is shown in Fig. 18. Figure 19 shows the bump shape. Since there are several excitation input due to the different length of the bump such as 1000 mm, 700 mm, and 40 mm, it can be shown that results of the proposed bushing model are different with Kelvin-Voight model. Figure 20 and 21 represent the vertical displacement and vertical acceleration of the chassis, respectively. In the figures, solid line means the proposed bushing model. Figure 22 and 23 show the bushing forces and FFTs of the bushing forces, respectively. This figure shows that the ranges of hysteretic response of the neural network bushing model are much wider than those of the linear bushing model. Therefore, the proposed bushing model would be useful for the

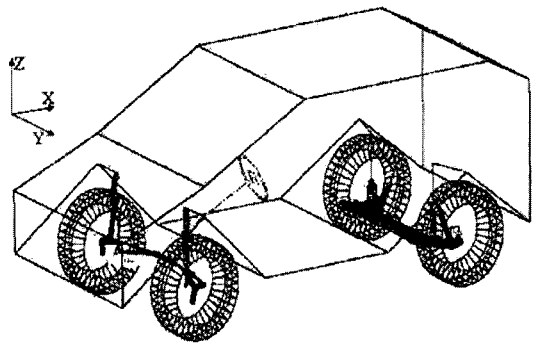

Fig. 17 Full-car model with the neural network bushing model

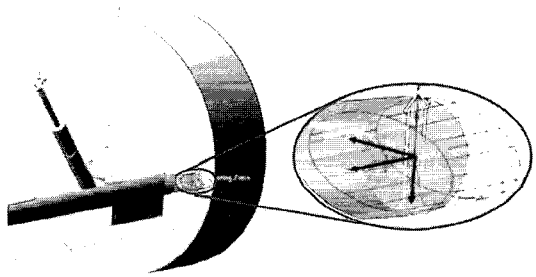

Fig. 18 Neural network bushing model

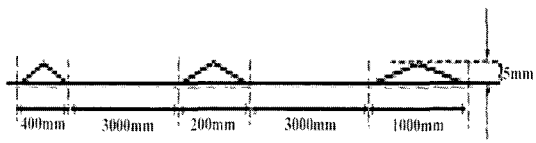

Fig. 19 Bump shape

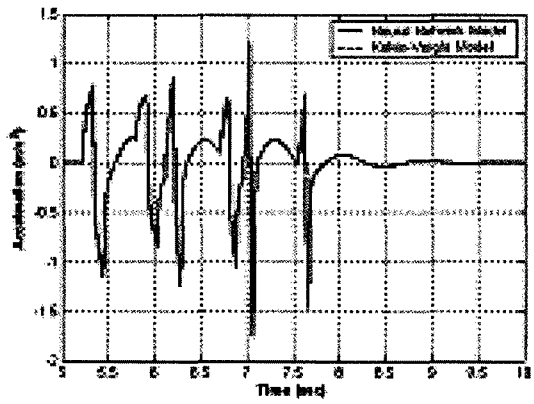

Fig. 20 Vertical displacement of a chassis

practical design and analysis of the vehicle suspension system.

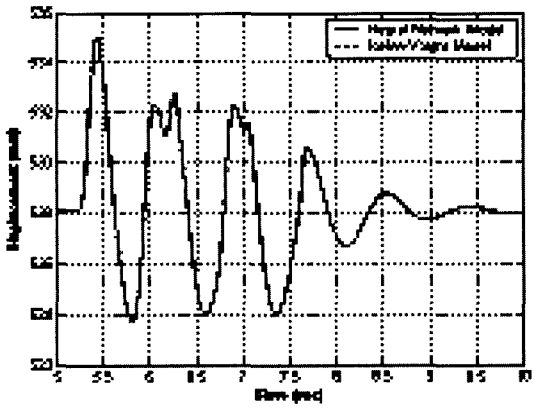

Fig. 21 Vertical acceleration of a chassis

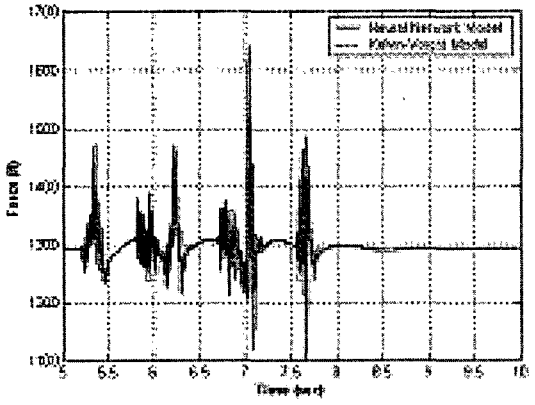

Fig. 22 Bushing force

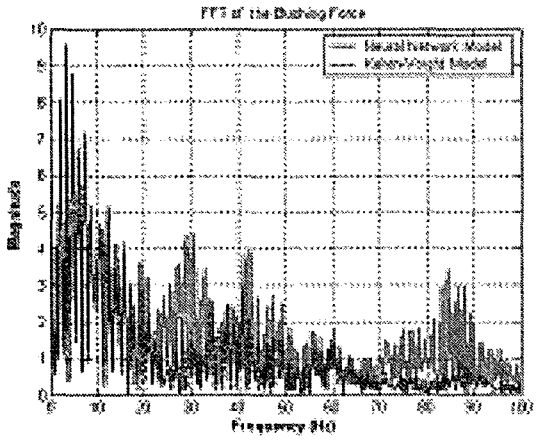

Fig. 23 FFT of a bushing force

5.2 Three-axis neural network bushing model

To do the vehicle simulation under the real vehicle environment, three-axis bushing model should be considered. Therefore, 3-axis neural bushing model was developed and shown in Fig. 24. In the 3-axis bushing model, three directional excitations were imposed and three direction output forces are obtained simultaneously. Figure 25 and 26 represent the axial direction (X) bushing force and bushing force vs displacement, respectively. Figure 27 and 28 represent the radial direction (Y) bushing force and bushing force vs

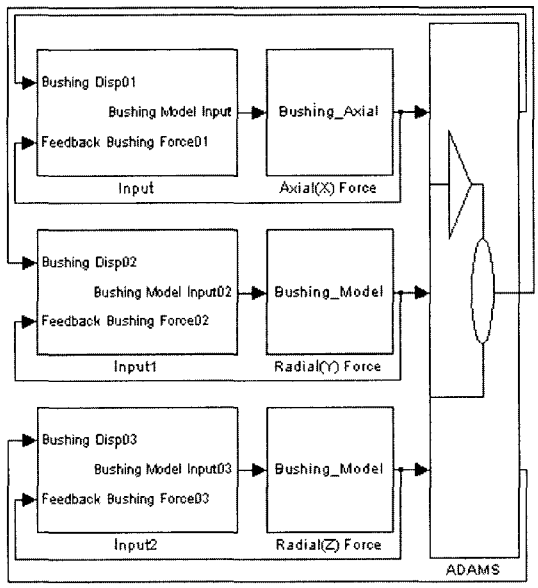

Fig. 24 Three-axis bushing model

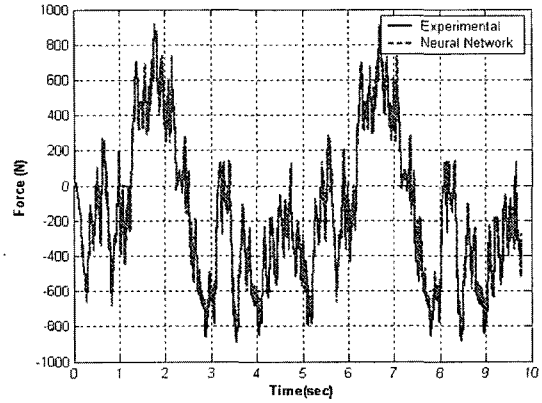

Fig. 25 Axial direction bushing force (x)

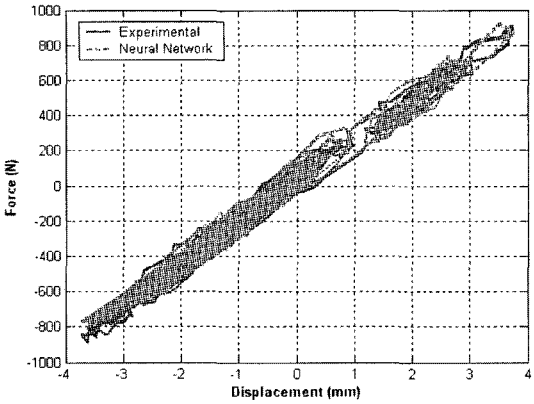

Fig. 26 Displacement vs. bushing force (x)

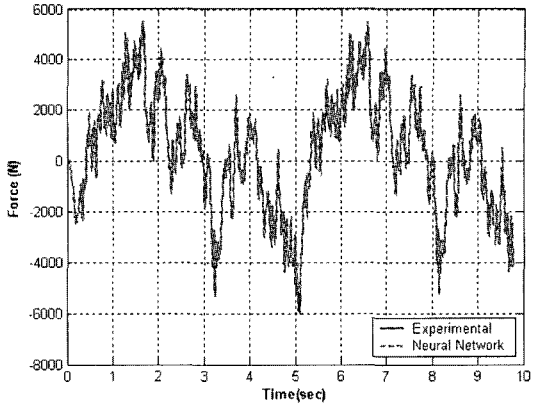

Fig. 29 Radial bushing force (z)

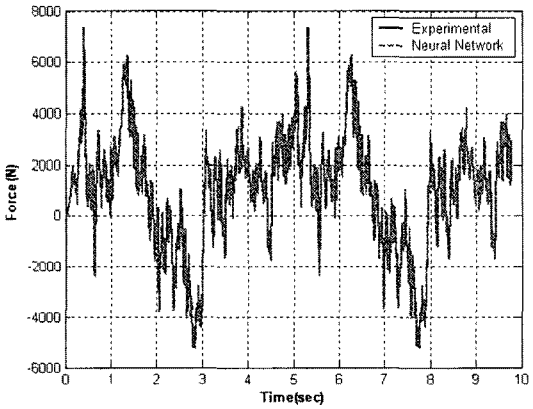

Fig. 27 Radial bushing force (y)

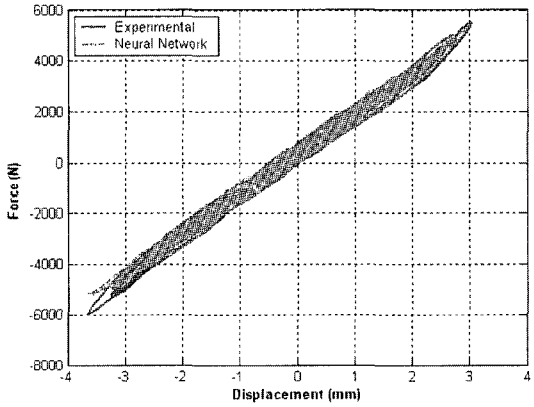

Fig. 30 Displacement vs. bushing force (z)

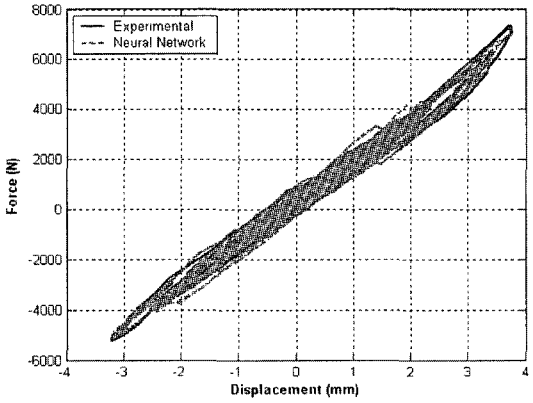

Fig. 28 Displacement vs. bushing force (y)

displacement, respectively. Figure 29 and 30 represent the radial direction (Z) bushing force and bushing force vs displacement, respectively. Three axis neural network bushing model will be used to do the handling simulations, etc.

6. Conclusion

A neural network bushing model for the practical vehicle dynamic analysis is proposed in this paper. The radial and axial tests using the MTS testing machine were carried out with varying the amplitude and the frequency of the excitation. From the test results, the hysteretic and nonlinear characteristics of the rubber bush were obtained. To model the rubber bushing featuring this hysteretic behavior for the vehicle dynamic analysis, an artificial neural network technique with a back propagation algorithm was adopted. Since the rubber bushing has hysteretic characteristics, the function of 'NARMAX' proposed by

Narendra was employed to construct the neural network algorithm. MATLAB and SIMULINK were used to construct the empirical bushing module. An interface module was developed to link MATLAB and ADAMS program. Dynamic simulation of the test rig using the proposed bushing model was verified to have a good agreement with experimental results. To demonstrate the feasibility of the proposed bushing model, a full-car dynamic model was simulated using the proposed bushing model.

Acknowledgment

The authors would like to thank the financial support by KOTEF (Korea Industrial Technology Foundation) through the graduate student education projects for regional strategic industries in Korea.

References

ADAMS, M. D. I., 1994, Version 8.0 User's Guide, Ann Arbor, MI, U.S.A..

Andrew J. Barber, 2000, "Accurate Models for Complex Vehicle Components using Empirical Methods," *SAE paper 2000-01-1625*.

Blundell, M. V., 1998, "The Influence of Rubber Bush Compliance on Vehicle Suspension Movement," *Materials and Design*, (19), pp. 29~37.

CADSI, 1995, DADS Revision 8.0 User's Manual, Oakdale, IA, U.S.A..

Fash, J. W., 1994 "Modeling of Shock Absorber Behavior using Artificial Neural Networks," *SAE 940248*.

Hoyong Kim, 1995, Paul I. Ro, "A Tire Side Force Model by Artificial Neural Network," *SAE paper 951051*.

Kuo, E. Y., 1997, "Testing and Characterization of Elastomeric Bushings for Large Deflection Behavior," *SAE paper*, No. 970099.

Narendra. K. S. and Parthasarathy, K., 1990, "Identification and Control of Dynamic System Using Neural Networks," *IEEE Transactions on Neural Networks*, 1(1), pp. 4~27.

Richard, C., 2003, Dorf, Control Analysis and MATLAB and SIMULINK Application.